



**Two-Dimensional Current Diffusion
in the Rails of a Railgun**

by John D. Powell and Alexander E. Zielinski

ARL-TR-4618

October 2008

NOTICES

Disclaimers

The findings in this report are not to be construed as an official Department of the Army position unless so designated by other authorized documents.

Citation of manufacturer's or trade names does not constitute an official endorsement or approval of the use thereof.

Destroy this report when it is no longer needed. Do not return it to the originator.

Army Research Laboratory

Aberdeen Proving Ground, MD 21005-5069

ARL-TR-4618

October 2008

Two-Dimensional Current Diffusion in the Rails of a Railgun

**John D. Powell and Alexander E. Zielinski
Weapons and Materials Research Directorate, ARL**

REPORT DOCUMENTATION PAGE			<i>Form Approved</i> OMB No. 0704-0188		
Public reporting burden for this collection of information is estimated to average 1 hour per response, including the time for reviewing instructions, searching existing data sources, gathering and maintaining the data needed, and completing and reviewing the collection information. Send comments regarding this burden estimate or any other aspect of this collection of information, including suggestions for reducing the burden, to Department of Defense, Washington Headquarters Services, Directorate for Information Operations and Reports (0704-0188), 1215 Jefferson Davis Highway, Suite 1204, Arlington, VA 22202-4302. Respondents should be aware that notwithstanding any other provision of law, no person shall be subject to any penalty for failing to comply with a collection of information if it does not display a currently valid OMB control number. PLEASE DO NOT RETURN YOUR FORM TO THE ABOVE ADDRESS.					
1. REPORT DATE (DD-MM-YYYY) October 2008		2. REPORT TYPE Final		3. DATES COVERED (From - To) October 2006–September 2007	
4. TITLE AND SUBTITLE Two-Dimensional Current Diffusion in the Rails of a Railgun			5a. CONTRACT NUMBER		
			5b. GRANT NUMBER		
			5c. PROGRAM ELEMENT NUMBER		
6. AUTHOR(S) John D. Powell and Alexander E. Zielinski			5d. PROJECT NUMBER AH75622618		
			5e. TASK NUMBER		
			5f. WORK UNIT NUMBER		
7. PERFORMING ORGANIZATION NAME(S) AND ADDRESS(ES) U.S. Army Research Laboratory ATTN: AMSRD-ARL-WM-TE Aberdeen Proving Ground, MD 21005-5069			8. PERFORMING ORGANIZATION REPORT NUMBER ARL-TR-4618		
9. SPONSORING/MONITORING AGENCY NAME(S) AND ADDRESS(ES)			10. SPONSOR/MONITOR'S ACRONYM(S)		
			11. SPONSOR/MONITOR'S REPORT NUMBER(S)		
12. DISTRIBUTION/AVAILABILITY STATEMENT Approved for public release; distribution is unlimited.					
13. SUPPLEMENTARY NOTES					
14. ABSTRACT We extend a previously developed, two-dimensional model for investigating current and heat transport in railguns. The new model permits the treatment of problems in which there are two components of the magnetic induction and a single component of the current density. In our previous models, there were two components of the current density and only one component of the magnetic induction. The basic mathematical formalism is developed and applied to a two-dimensional configuration in rectangular coordinates. The model is then used to investigate current diffusion into a pair of parallel rails such as might be appropriate in a railgun behind the projectile. The calculations produce the time and spatial distributions of the electromagnetic fields within the rails. Some physical discussion of the results is provided.					
15. SUBJECT TERMS railgun, current diffusion, electromagnetic propulsion, electrodynamics, Maxwell's equations					
16. SECURITY CLASSIFICATION OF:			17. LIMITATION OF ABSTRACT UL	18. NUMBER OF PAGES 28	19a. NAME OF RESPONSIBLE PERSON John D. Powell
a. REPORT UNCLASSIFIED	b. ABSTRACT UNCLASSIFIED	c. THIS PAGE UNCLASSIFIED			19b. TELEPHONE NUMBER (Include area code) 410-278-5783

Contents

List of Figures	iv
List of Tables	iv
Acknowledgments	v
1. Introduction	1
2. Model and Formalism	3
2.1 Vector Potential Formulation in Three Dimensions.....	3
2.2 Governing Equations for 2-D Rectangular Coordinates	4
2.3 Boundary Conditions.....	6
2.4 Generalized Coordinates	6
2.5 Numerical Procedure.....	8
3. Calculations	8
4. Summary and Future Work	15
5. References	16
Distribution List	18

List of Figures

Figure 1. X-Y cross section of rails.	1
Figure 2. Domain and grid employed in the calculation.....	9
Figure 3. Actual and calculated current as a function of time.	11
Figure 4. Vector potential contours at 5 ms.	12
Figure 5. Current density contours at different times.	13
Figure 6. Temperature contours at different times.....	14

List of Tables

Table 1. Properties for copper employed in calculations (SI units are used unless otherwise noted).....	11
Table 2. Inductance per unit length at various times.	15

Acknowledgments

The authors are grateful to Dr. Casey Uhlig for his thoughtful review of this report and to Dr. Charles Hummer for comparing our results to results from some of his model calculations.

INTENTIONALLY LEFT BLANK.

1. Introduction

In previous work (Powell et al., 1993; Powell and Zielinski, 1995, 1997, 1999, 2001, 2003, 2004), we have developed a number of two-dimensional (2-D) models for solving coupled Maxwell and energy transport equations in two dimensions. The models have been used to investigate current and heat transport in the rail and armature of both solid- and plasma-armature railguns. All of these calculations have been based upon the assumption that the rail height h is very large when compared to the rail separation w (see figure 1). The models are known to predict values of the in-bore fields and armature acceleration that are too large when compared to realistic experimental values for finite-rail-height launchers. Some methods for scaling the results to make them more realistic have also been studied (Powell and Zielinski 1995, 1997, 2004).

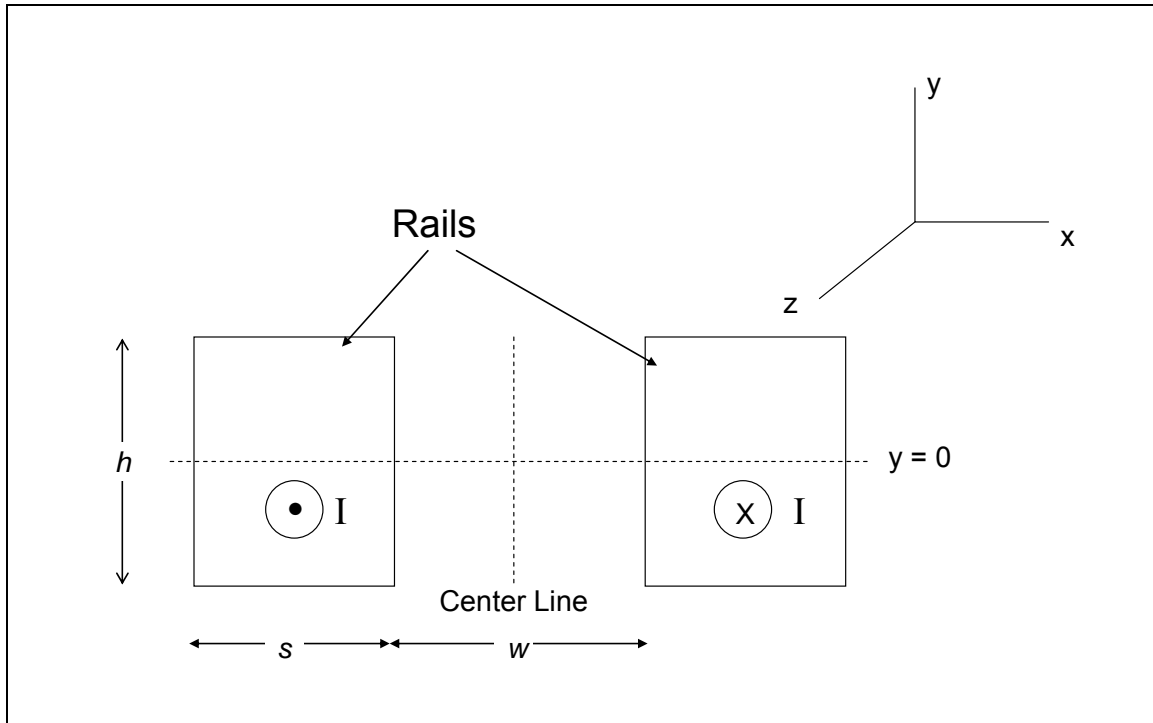


Figure 1. X-Y cross section of rails.

When the rail height is infinitely large, there exists only one component of the magnetic induction (along the direction of the rail height) and two components of the electric field and current density (along directions normal to the rail height). In this report, we consider the “alternate” 2-D model in which the current is conducted only in one direction, while the magnetic induction has two components. The model should provide us with a methodology for considering a number of different problems that were not possible with our previous model.

Such problems include, for example, electromagnetic (EM) field transport in finite-height rails at distances far removed from the armature. At these distances, we expect that current is conducted only along the direction of the rail, but that the magnetic induction field will “wrap around” the rail. Consequently, there will exist only one component of the current density (along the rail direction) but two components of the magnetic induction (along directions normal to the rail direction). We should also point out that we have recently extended a similar model in cylindrical coordinates that was used to investigate the disruption of shaped charge jets by axially directed currents. That model has now been used to study current diffusion in some fairly complicated cylindrical geometric configurations in another report (Powell, 2008).

In our previous work, we solved Maxwell’s equations directly for the EM fields, but in this report we employ the formalism of the vector and scalar potentials. This approach is used because there is a single component of the vector potential from which the EM fields follow easily. The calculations can therefore be significantly simplified; the two approaches yield similar results.

Very complex models and computer codes for doing similar types of calculations have been developed in the past by others. The most noteworthy example for application to railguns is perhaps the simulation code EMAP3D (Electromechanical Analysis Program in Three Dimensions) (Hsieh, 1995). That code, which is three dimensional, has the capability of undertaking the sorts of problems of interest to us. Our intent, however, is to develop a simpler model with which we can undertake elementary calculations and that can be extended to more complicated studies in the future. Two-dimensional models that are similar to the one developed here include models by Kerrisk (1982), who investigated current diffusion in the rails of a railgun, and by Freeman (1988), who studied the launch of projectiles with a reconnection gun.

The primary purpose of the report is to develop the model and to provide the methodology necessary for undertaking future calculations. One simple example, however, is calculated. The example is concerned with the diffusion of current and the resulting ohmic heating of two long parallel rails that carry current only along the direction of the rails. This problem has potential importance for investigating rail erosion and assessing effects that might contribute to transition. We also undertake a calculation of the inductance per unit length L' of the pair of rails.

The organization of the report is as follows. In section 2, we derive the general governing equations in three dimensions and then obtain the limiting results for a 2-D, Cartesian model. Some of this analysis was contained in our previous report (Powell, 2008), but it is also included here for completeness. In section 3, we undertake the current diffusion calculation just described. Finally, section 4 contains a summary and indicates possible future directions for this research.

2. Model and Formalism

We consider one or more electrical conductors contained within some domain \mathcal{D} . The conductors carry current, which may be specified a priori or may need to be calculated. The conductors may be either in a solid or liquid state, and they may be moving with a velocity \vec{v} . We do neglect internal motion, however, so that the conductors move as perfectly rigid bodies. Our intent is to determine the EM fields throughout the domain as well as the temperature of the conductors as a function of both space and time.

2.1 Vector Potential Formulation in Three Dimensions

We begin with Maxwell's equations and Ohm's law in three dimensions. Let \vec{E} , \vec{B} , \vec{v} , and \vec{J} be the electric field intensity, the magnetic induction field, the velocity of the conductor, and the current density, respectively. Let μ and σ be the permeability and electrical conductivity, respectively. Then we have

$$\nabla \times \vec{E} = -\frac{\partial \vec{B}}{\partial t}, \quad (1)$$

$$\nabla \times (\vec{B} / \mu) = \vec{J}, \quad (2)$$

$$\vec{J} = \sigma(\vec{E} + \vec{v} \times \vec{B}), \quad (3)$$

and

$$\nabla \cdot \vec{B} = 0. \quad (4)$$

These equations are written in the low-frequency approximation, which applies whenever the velocity v is small when compared to the light speed c_0 , and all relevant time scales in the problem are long when compared to $(\mu\sigma c_0^2)^{-1}$. Both conditions are easily met in the electrical conduction problems that we consider. It is also assumed that the relationship between the magnetic field intensity \vec{H} , which strictly should appear in equation 2, and the magnetic induction \vec{B} is given by $\vec{H} = \vec{B} / \mu$, where μ is assumed to be constant within the material.

We now define the vector potential \vec{A} by the relation

$$\vec{B} = \nabla \times \vec{A}. \quad (5)$$

With this definition, it is apparent that equation 4 is satisfied automatically, since the divergence of the curl of any vector is always zero. Substitution of equation 5 into equation 1 then provides

$$\nabla \times \left(\vec{E} + \frac{\partial \vec{A}}{\partial t} \right) = 0. \quad (6)$$

This equation has the solution

$$\vec{E} + \frac{\partial \vec{A}}{\partial t} = -\nabla \phi, \quad (7)$$

where $\nabla \phi$ is an arbitrary function that constitutes the scalar potential contribution to the electric field.

We finally observe that specification of the curl of \vec{A} as given in equation 5 does not specify the vector uniquely. A unique specification can be obtained, however, if we also indicate the divergence of the vector. A convenient choice (there are others), which is known as the Coulomb gauge, is

$$\nabla \cdot \vec{A} = 0. \quad (8)$$

If we assume this condition, substitute equations 3, 5, and 7 into equation 2, and expand, we obtain

$$\sigma \frac{\partial \vec{A}}{\partial t} = \frac{1}{\mu} \nabla^2 \vec{A} - \nabla(1/\mu) \times \nabla \times \vec{A} + \sigma(\vec{v} \times \nabla \times \vec{A}) - \sigma \nabla \phi, \quad (9)$$

where by definition $\nabla^2 \vec{A} = \nabla^2 A_x \hat{i} + \nabla^2 A_y \hat{j} + \nabla^2 A_z \hat{k}$. Equation 9, solved with appropriate boundary conditions and a specification of $\nabla \phi$, permits determination of \vec{A} . Substitution of that result in equations 7, 5, and 3 then produces the remaining variables \vec{E} , \vec{B} , and \vec{J} . It should also be pointed out that equation 8 holds not only in the conductors but in the surrounding vacuum as well, provided we take $\sigma = 0$.

2.2 Governing Equations for 2-D Rectangular Coordinates

For the 2-D case with rectangular coordinates, we assume that all variables depend only on x and y and not on the coordinate z . Furthermore, for the specific case under study here, we assume that $\vec{A} = A \hat{z}$, $\vec{E} = E \hat{z}$, and $\vec{J} = J \hat{z}$. It is evident, then, from equation 5 that \vec{v} and \vec{B} may have components in both the x and y directions. If we furthermore note that equation 8 has only a z component, we must have that $\frac{\partial \phi}{\partial x} = \frac{\partial \phi}{\partial y} = 0$. Consequently, the only nonzero component of $\nabla \phi$ can be represented as $E_0(t)$, where E_0 is a position-independent function. If we now expand equation 9 completely, we find for the 2-D equation governing the evolution of \vec{A} the result

$$\sigma \left(\frac{\partial A}{\partial t} + u \frac{\partial A}{\partial x} + w \frac{\partial A}{\partial y} + E_0 \right) = \frac{1}{\mu} \left(\frac{\partial^2 A}{\partial x^2} + \frac{\partial^2 A}{\partial y^2} \right) - \frac{1}{\mu^2} \left(\frac{\partial \mu}{\partial x} \frac{\partial A}{\partial x} + \frac{\partial \mu}{\partial y} \frac{\partial A}{\partial y} \right). \quad (10)$$

In this equation, u and w represent the x and y components of the velocity, respectively. Once equation 10 has been solved for the vector potential A , we can determine the magnetic induction and current density from equations 5, 3, and 7. For the 2-D case, we have

$$B_x = \frac{\partial A}{\partial y}, \quad (11)$$

$$B_y = -\frac{\partial A}{\partial x}, \quad (12)$$

and

$$J = -\sigma \left(\frac{\partial A}{\partial t} + E_0 + u \frac{\partial A}{\partial x} + w \frac{\partial A}{\partial y} \right). \quad (13)$$

In general, the electrical conductivity σ depends sensitively on the temperature of the conductors. Consequently, it is necessary to solve an energy transport equation within the conducting regions in order to determine the temperature as a function of space and time. We account for ohmic heating and ordinary heat conduction, and we allow for melting but no other phase change. Let e , C , ρ , and κ be the specific internal energy, the specific heat capacity, the density, and the thermal conductivity, respectively. Let T_m be the melting temperature, and let H_f be the latent heat of fusion. We then assume that the time evolution of the energy is given by

$$\rho \frac{\partial e}{\partial t} + \rho u \frac{\partial e}{\partial x} + \rho w \frac{\partial e}{\partial y} = \kappa \frac{\partial^2 T}{\partial x^2} + \kappa \frac{\partial^2 T}{\partial y^2} + \frac{\partial \kappa}{\partial x} \frac{\partial T}{\partial x} + \frac{\partial \kappa}{\partial y} \frac{\partial T}{\partial y} + J^2 / \sigma. \quad (14)$$

The first four terms on the right-hand side account for heat conduction, whereas the last term accounts for ohmic heating.

The relationship between e and T must be determined by an equation of state, and we use the simple representation

$$e = \int_0^T C(T') dT' + H_f \Theta(T - T_m). \quad (15)$$

In this equation, Θ is the Heaviside function, which is equal to zero when T is less than T_m and is equal to unity otherwise. The equation clearly predicts that melting occurs at a well-defined temperature T_m . Since the energy depends on ohmic heating and the electrical conductivity depends on temperature, there is an obvious coupling between equations 10 and 14.

2.3 Boundary Conditions

Boundary conditions that must be applied at the outer edges of the domain \mathcal{D} are determined by physical considerations for each problem considered. There are, however, additional boundary conditions that must hold at the interface between the conductors and the vacuum. For the vector potential A , these conditions can be obtained by integrating equations 2 and 4 across such an interface of thickness δ and then taking the limit as $\delta \rightarrow 0$. Let \hat{n} be the unit normal to the interface. Then, if we assume that there are no surface currents, the integrations yield

$$\hat{n} \bullet \{\vec{B}\} = 0 \quad (16)$$

and

$$\hat{n} \times \{\vec{B} / \mu\} = 0, \quad (17)$$

where the braces are used (in this section only) to denote the change in the quantity in question as the interface is crossed. Thus, in accordance with standard results, we have that the normal component of \vec{B} and the tangential component of \vec{H} are continuous at the boundary. In terms of the vector potential A , equation 16 implies that A is continuous at the boundary, whereas equation 17 implies that

$$n_x \left\{ \frac{1}{\mu} \frac{\partial A}{\partial x} \right\} + n_y \left\{ \frac{1}{\mu} \frac{\partial A}{\partial y} \right\} = 0. \quad (18)$$

Thus if μ is discontinuous at the boundary, so too is the normal derivative of A .

Since heat conduction is accounted for, there must also be boundary conditions on the temperature at the conductor surfaces. The appropriate condition can also be obtained by integrating equation 14 across the boundary. We obtain

$$\vec{n} \bullet \{\kappa \nabla T\} = 0. \quad (19)$$

Therefore, since κ is zero in the vacuum, equation 19 produces the usual result that the normal derivative of T must vanish at a conductor-vacuum interface.

2.4 Generalized Coordinates

As in previous work, we often find it convenient to transform the governing equations to a set of generalized coordinates. The purpose of this transformation is to map a complicated physical space into a much simpler computational space in which the calculations are performed. The computational space is chosen to be rectangular. This procedure makes it possible to consider irregularly shaped boundaries, for example, in a rather straightforward manner. Once the computation has been completed, the results are then “transformed back” to the physical space for presentation.

We now outline the general procedure for performing the transformation. Greater detail can be found in our previous work (Powell and Zielinski, 1997) or in various textbooks (Anderson et al., 1984; Hoffmann, 1989). We denote the physical coordinates by (x,y,t) and the computational coordinates by (ξ,η,τ) , and we write quite generally

$$\begin{aligned}\xi &= \xi(x, y, t) \\ \eta &= \eta(x, y, t) \\ \tau &= t.\end{aligned}\tag{20}$$

The partial derivatives that appear in equations 10 and 14 must be expressed in terms of the computational coordinates, and the appropriate relations can be obtained from the chain rule. We have for any function F

$$\begin{aligned}F_x &= F_\xi \xi_x + F_\eta \eta_x \\ F_y &= F_\xi \xi_y + F_\eta \eta_y \\ F_{xx} &= F_\xi \xi_{xx} + F_\eta \eta_{xx} + \xi_x^2 F_{\xi\xi} + \eta_x^2 F_{\eta\eta} + 2\xi_x \eta_x F_{\xi\eta} \\ F_{yy} &= F_\xi \xi_{yy} + F_\eta \eta_{yy} + \xi_y^2 F_{\xi\xi} + \eta_y^2 F_{\eta\eta} + 2\xi_y \eta_y F_{\xi\eta} \\ F_t &= F_\tau.\end{aligned}\tag{21}$$

We have used here (this section only) subscripts that are coordinates to denote partial derivatives with respect to those coordinates. Consequently, $\eta_{xx} = \partial^2 \eta / \partial x^2$, $F_{\xi\xi} = \partial^2 F / \partial \xi^2$, and so forth.

We now substitute from equation 21 into equations 10 and 14 to produce in terms of the computational variables

$$\begin{aligned}\sigma[A_\tau + u(A_\xi \xi_x + A_\eta \eta_x) + w(A_\xi \xi_y + A_\eta \eta_y) + E_0] \\ = (1/\mu)[A_\xi(\xi_{xx} + \xi_{yy}) + A_\eta(\eta_{xx} + \eta_{yy}) \\ + A_{\xi\xi}(\xi_x^2 + \xi_y^2) + A_{\eta\eta}(\eta_x^2 + \eta_y^2) + 2(\xi_x \eta_x + \xi_y \eta_y)A_{\xi\eta}] \\ - (1/\mu^2)[(\mu_\xi \xi_x + \mu_\eta \eta_x)(A_\xi \xi_x + A_\eta \eta_x) \\ + (\mu_\xi \xi_y + \mu_\eta \eta_y)(A_\xi \xi_y + A_\eta \eta_y)] ,\end{aligned}\tag{22}$$

and

$$\begin{aligned}\rho[e_\tau + u(e_\xi \xi_x + e_\eta \eta_x) + w(e_\xi \xi_y + e_\eta \eta_y)] \\ = \kappa[T_\xi(\xi_{xx} + \xi_{yy}) + T_\eta(\eta_{xx} + \eta_{yy}) \\ + T_{\xi\xi}(\xi_x^2 + \xi_y^2) + T_{\eta\eta}(\eta_x^2 + \eta_y^2) + 2(\xi_x \eta_x + \xi_y \eta_y)T_{\xi\eta}] \\ + [(\kappa_\xi \xi_x + \kappa_\eta \eta_x)(T_\xi \xi_x + T_\eta \eta_x) \\ + (\kappa_\xi \xi_y + \kappa_\eta \eta_y)(T_\xi \xi_y + T_\eta \eta_y) + J^2 / \sigma].\end{aligned}\tag{23}$$

As is generally the case in these types of transformations, the transformed equations are much more complicated than the original ones.

Our earlier work (Powell and Zielinski, 1997, 2001) contained both complicated and simple transformations as indicated in equation 20 in order to achieve some desired mapping. For the problem to be considered here, only the trivial transformation

$$\begin{aligned}\xi &= y \\ \eta &= x\end{aligned}\tag{24}$$

is required. Consequently, we do not discuss the details of more complicated transformations and refer the reader to the references cited previously.

2.5 Numerical Procedure

We employ a numerical procedure similar to that which we have used in previous work. In particular, a rectangular computational grid with variable grid spacing in both directions is constructed. The spacing of grid points is chosen so that when the mapping to the physical space is effected, the grid will be small in regions for which we expect a strong spatial variation and larger in regions where we expect a more gradual variation. The derivatives in equations 22 and 23 are then represented by standard finite differences, and the equations, which may be nonlinear, are solved by a modified Newton-Raphson method (Ames, 1977).

3. Calculations

We now employ the previous model and formalism to undertake one reasonably simple calculation. The calculation is concerned with electrical conduction in a segment of the rails of a railgun. The segment is assumed to be sufficiently far behind the projectile that the current I is conducted only in the z direction. If we view a cross section in the x - y plane, the configuration appears as shown in figure 1. The rail on the left conducts current in the positive z direction, while the rail on the right provides the return current path. The rails have height h , separation w , and thickness s , given by 34, 44, and 19.2 mm, respectively. It is evident from the figure that there is symmetry about $y = 0$, as well as about the vertical centerline indicated. Consequently, we need only consider one quadrant of the configuration shown and choose, for convenience, the upper left-hand quadrant.

Shown in figure 2 are the grid and domain \mathcal{D} for the calculation. The grid shown is the grid in the physical space, but it is equivalent to the computational grid because of the transformation indicated in equation 24. The origin of the x axis was chosen to lie at the left-hand side of the domain. Also shown in the figure are the boundary conditions that are assumed to hold on the edges of the domain. The top and left-hand sides are assumed to be sufficiently far from the rails that we can assume that $A = 0$. From symmetry considerations, we also have $A = 0$ along the right-hand side (the centerline in figure 1) and $\partial A / \partial y = 0$ along $y = 0$.

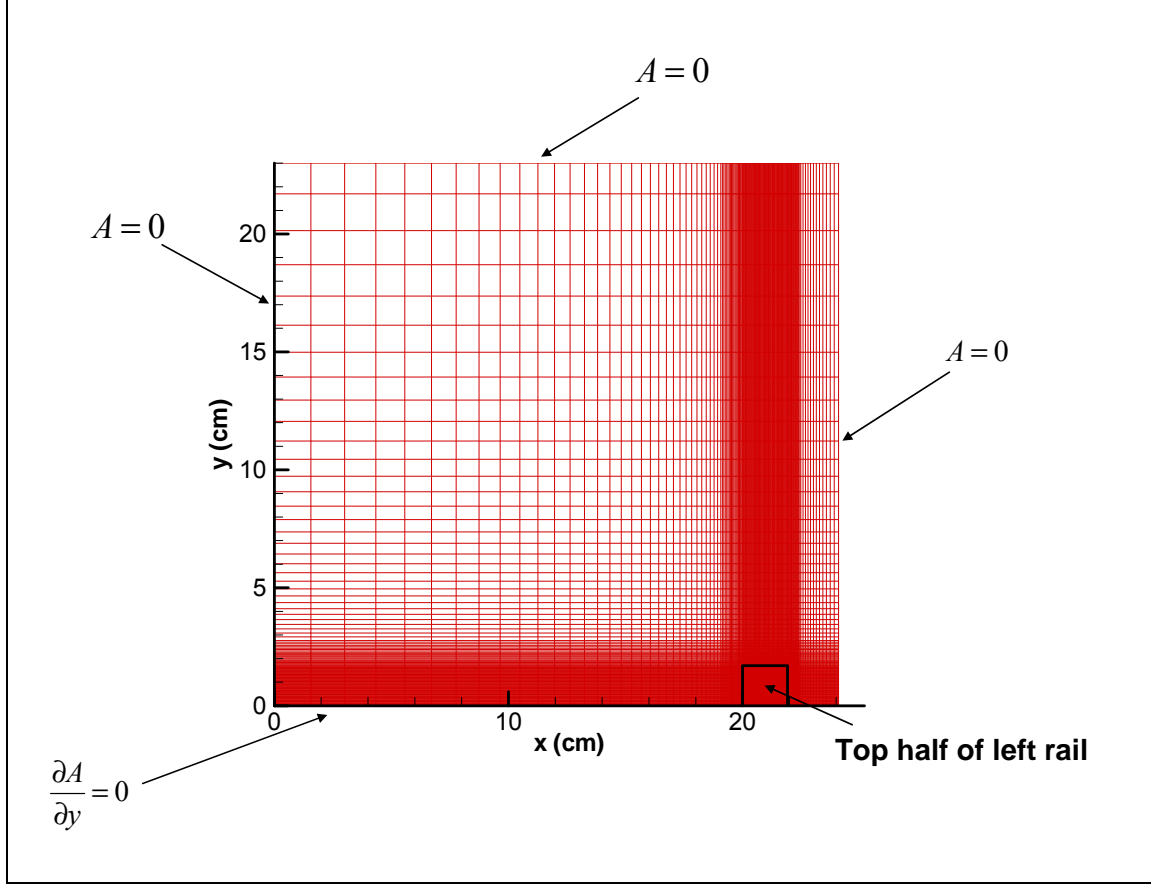


Figure 2. Domain and grid employed in the calculation.

For simplicity, we had intended to impose a constant total current of I_0 for all calculations. However, in order to avoid discontinuities in either the current or its derivatives, we assumed a variation of the form

$$I = I_0 \tanh(t/t_0) \quad (25)$$

and chose t_0 be small when compared to the total calculation time. The asymptotic value of this functional form is I_0 , and I/I_0 is greater than 0.95 when $t/t_0 = 2$.

It is then necessary to determine the relationship between the total current I and the parameter E_0 that appears in equation 10. The most straightforward way is to integrate equation 13 over the cross-sectional area of the rail and equate the result to the total current I . A somewhat simpler expression can be obtained, however, if we note from equation 10 that the current density J can also be written as

$$J = -\frac{1}{\mu} \nabla \cdot \nabla A, \quad (26)$$

where we have assumed that the permeability is constant in the conductors. If we now exploit the divergence theorem to evaluate the required integral, we have

$$\oint \frac{\partial A}{\partial n} dl = -\mu I / 2, \quad (27)$$

where $\partial A / \partial n$ denotes the normal derivative of A at the boundary, and where the integral is to be evaluated over the boundaries of the rail cross section. The procedure is standard and has been discussed, for example, by Hoffmann (1989). The factor of 2 appears on the right-hand side because only the top half of the rail is included in the domain. By using the divergence theorem, we have converted a 2-D integral to a series of three one-dimensional integrals. Simpson's rule is used to perform the integrations.

The constraint imposed by equation 27 should be sufficient to determine E_θ . It has proved, however, to be enormously difficult to implement this relationship in our computer code and to obtain accurate, stable values for E_θ . Ultimately, we have resorted to the time-consuming procedure of assuming a value for E_θ at some particular time step, obtaining convergence of equations 10 and 14, and then calculating a value for the total current, denoted by I_c . We then changed E_θ and recomputed. This process allowed us to find the acceptable value of E_θ —i.e., the one that produced $I = I_c$ —by the procedure of bracketing and bisection (Press et al., 1986). Even then, however, we sometimes found small oscillations in E_θ as a function of time. When these small oscillations occurred, we fit E_θ to a curve, typically represented by a three-parameter exponential of the form

$$E_\theta = a + be^{-ct}, \quad (28)$$

where a , b , and c are constants, and recomputed. Usually, we could then obtain reasonable agreement between the computed and imposed current. This laborious procedure is not entirely satisfactory, but we have been unable thus far to produce something more suitable. The difficulty of obtaining E_θ for situations in which a total current is to be specified has been experienced and discussed by others (Freeman, 1988).

We have performed calculations for a number of different values of I_0 as well as for a number of different conditions. We discuss only one, however. For this particular calculation we chose $I_0 = 500$ kA, $t_0 = 100$ μ s, and assumed that the imposed current was represented by equation 25. The temperature-dependent thermophysical properties for the copper rails, shown in table 1, were employed. The permeability μ was assumed to be constant and equal to its free-space value μ_0 everywhere.

We followed the previously discussed procedure to determine the value of E_0 by fitting the numerical results to an exponential. Approximate values of the constants were given by: $a = -16.3 \text{ V/m}$, $b = -2.14 \times 10^3 \text{ V/m}$, and $c = 1.34 \times 10^4 \text{ s}^{-1}$.

Table 1. Properties for copper employed in calculations
(SI units are used unless otherwise noted).

Property	Value
C	$360.0 + 0.1T$
κ	$412.0 - 0.07887T$
ρ	8900.0
σ^{-1} ($\mu\Omega\text{-cm}$)	$-0.542 + 0.00781T$

The calculation was then repeated with this value of E_0 and produced the results for the computed current I_c shown in figure 3; the actual current I , given by equation 25, is also shown for comparison. The agreement is reasonable.

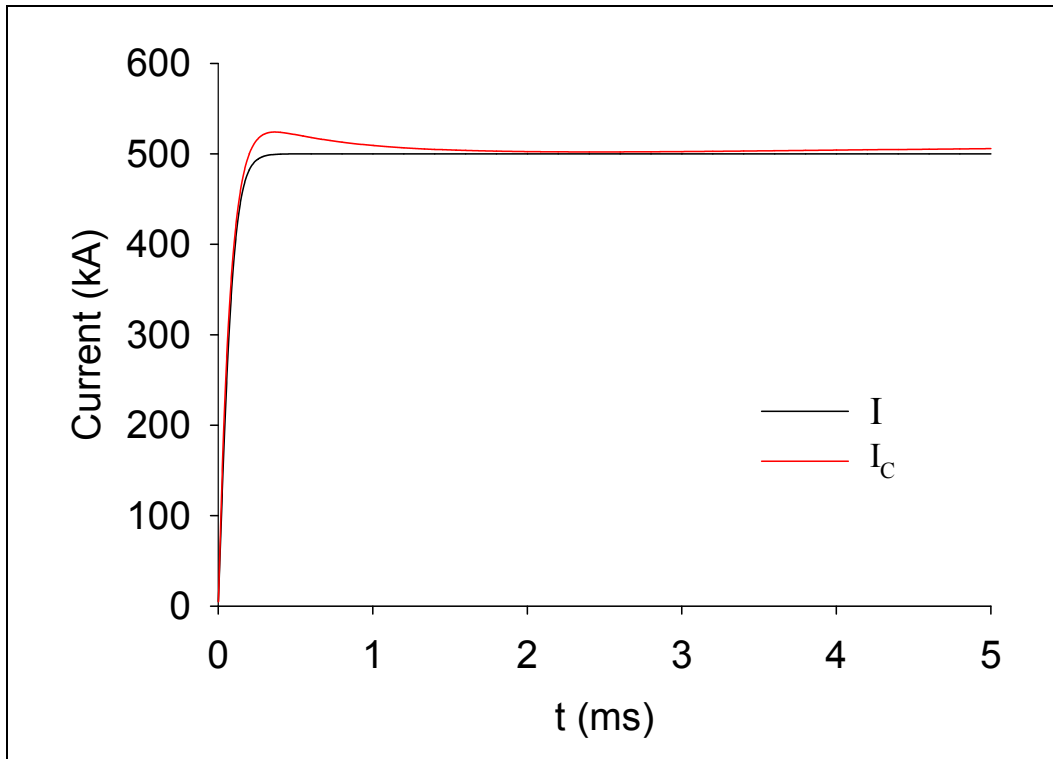


Figure 3. Actual and calculated current as a function of time.

The first results we show are the vector potential contours at the termination of the calculation at 5 ms. These contours are shown for the domain \mathcal{D} in figure 4; they can be sequentially reflected about the lines indicated to produce somewhat obvious results in all four quadrants. It is possible to prove (Powell, 2007) that the vector \vec{B} is tangent to lines of constant A . Thus the arrows in the figure indicate the direction of the magnetic induction at the points indicated. The magnitude of B_y varies inversely with the separation of the contour lines in the x direction, whereas the magnitude of B_x varies inversely with the separation in the y direction. Consequently, the B field “wraps around” the rails, but it is larger within the bore than it is outside. This effect is a consequence of finite rail height and was not seen in our previous models for which the rail height was infinite. It is also of some interest to compare the maximum value of B_y in the bore with the value obtained for an infinite rail height model. The maximum value of B_y occurs at $y = 0$ and at the inner surface of the rail ($x \approx 22$ cm); its value there is about 8.2 T. For the infinite rail height case, B_y is constant in the bore and its value is given by $B_y = \mu j$, where j represents the current per unit rail height. For $j \approx 15$ MA/m, we find $B_y \approx 19$ T for the infinite rail height case. There is, therefore, a difference of about a factor of 2 for the two cases.

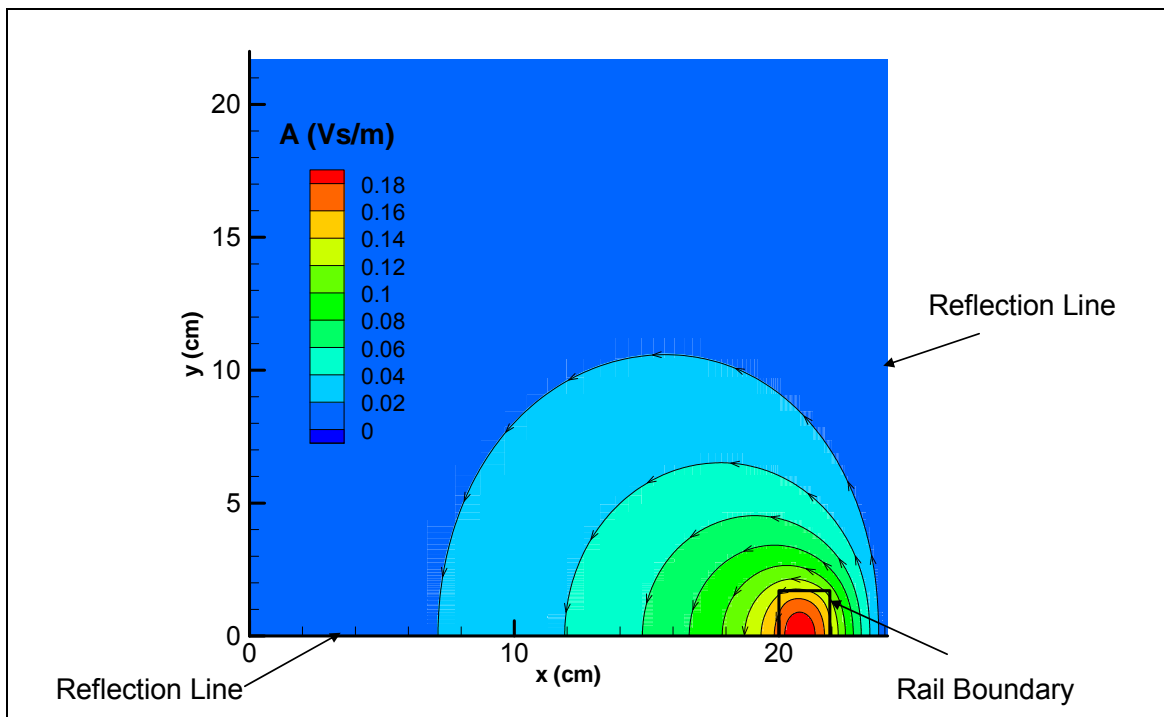


Figure 4. Vector potential contours at 5 ms.

We next show results for the temperature and current density within the rail at several times during the calculation. The current density is shown in figure 5. As expected, current begins to flow just inside the boundaries of the conductor where the gradients in the magnetic induction are largest. The magnitude is particularly high near the corners where both $\partial B_x / \partial y$ and

$\partial B_y / \partial x$ are large initially. On average, the magnitude is also higher on the right-hand side of the rail than it is on the left-hand side. This difference results because of the proximity of the return current rail on the right. As time progresses, the current diffuses inward from the sides and from the top of the rail. At late times, the current becomes fairly uniform within the rail as diffusion nears completion. The magnitude of the current density at these late times is near 80 kA/cm^2 , i.e., the total current divided by the cross-sectional area of the rail. An approximate time for diffusion to occur can be obtained from the standard skin-depth formula, $\delta_0 = (\pi / (\mu\sigma))^{1/2}$. If we assume that $\delta_0 = 1 \text{ cm}$, i.e., the half-thickness of the rail, and take σ^{-1} to be its room-temperature value of about $1.8 \mu\Omega\text{-cm}$, we obtain a time of about 2 ms. That result seems consistent with results in figure 5.

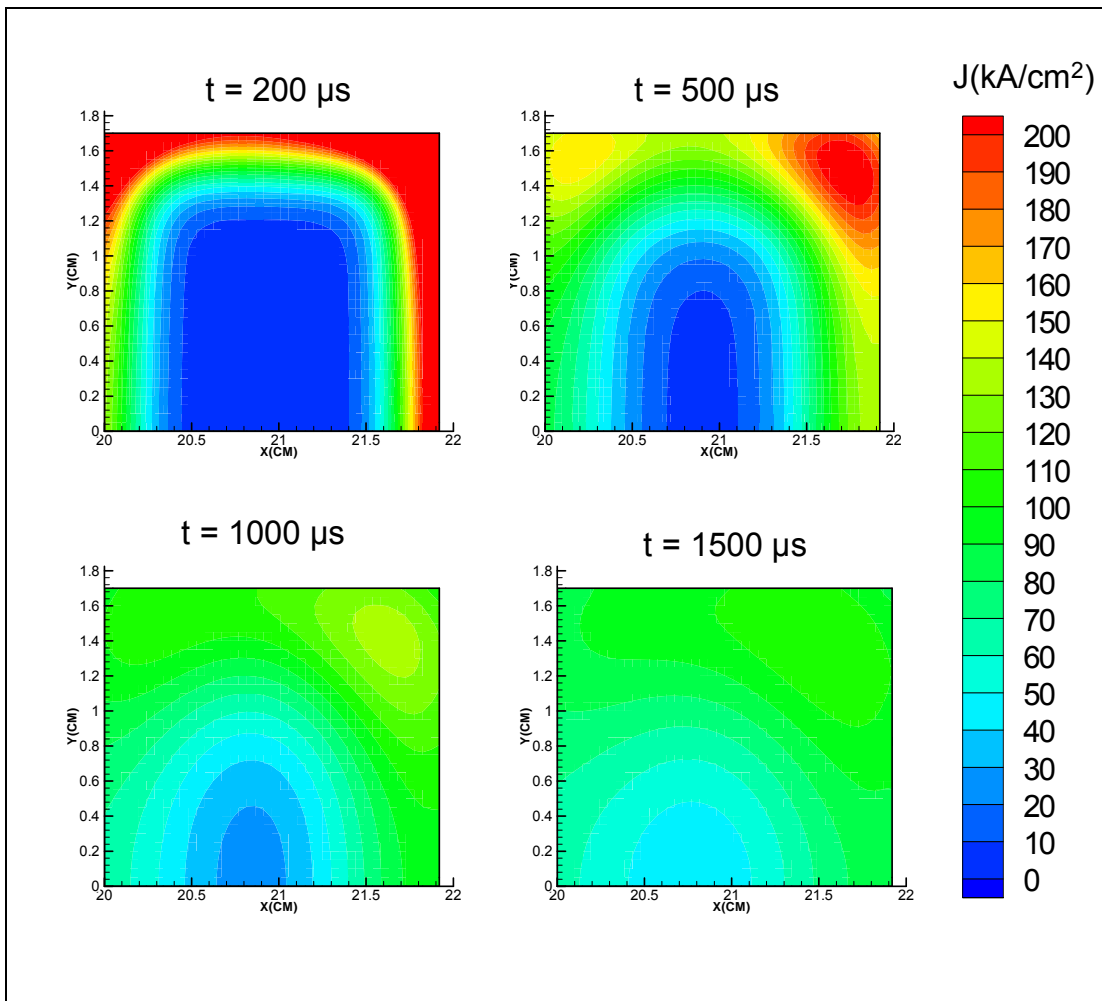


Figure 5. Current density contours at different times.

The isotherms, shown in figure 6, look somewhat similar to the current density contours. As the current diffuses inward, the rails are heated ohmically, but temperature increases lag the increase in current density. Furthermore, the temperature at any given point appears to rise monotonically with time. This behavior indicates that ohmic heating is much more significant than thermal conduction, an effect that is small both because of the relatively short time scale and the small temperature gradients. It is perhaps surprising that the temperature rise at the surface of the rails (only a few tens of degrees) is so small. Our previous calculations with the infinite rail height models have indicated substantially higher temperatures in the rails. The difference here can be attributed to two factors. First, the current per unit rail height in this case is smaller than in most of our previous work, and the initial temperature rise at the rail surface varies roughly as j^2 . Second, some significant rail heating occurs because of the velocity skin effect during the time that the trailing edge of the armature is near a given point on the rail surface. That effect is accounted for in our previous calculations but not in this one.

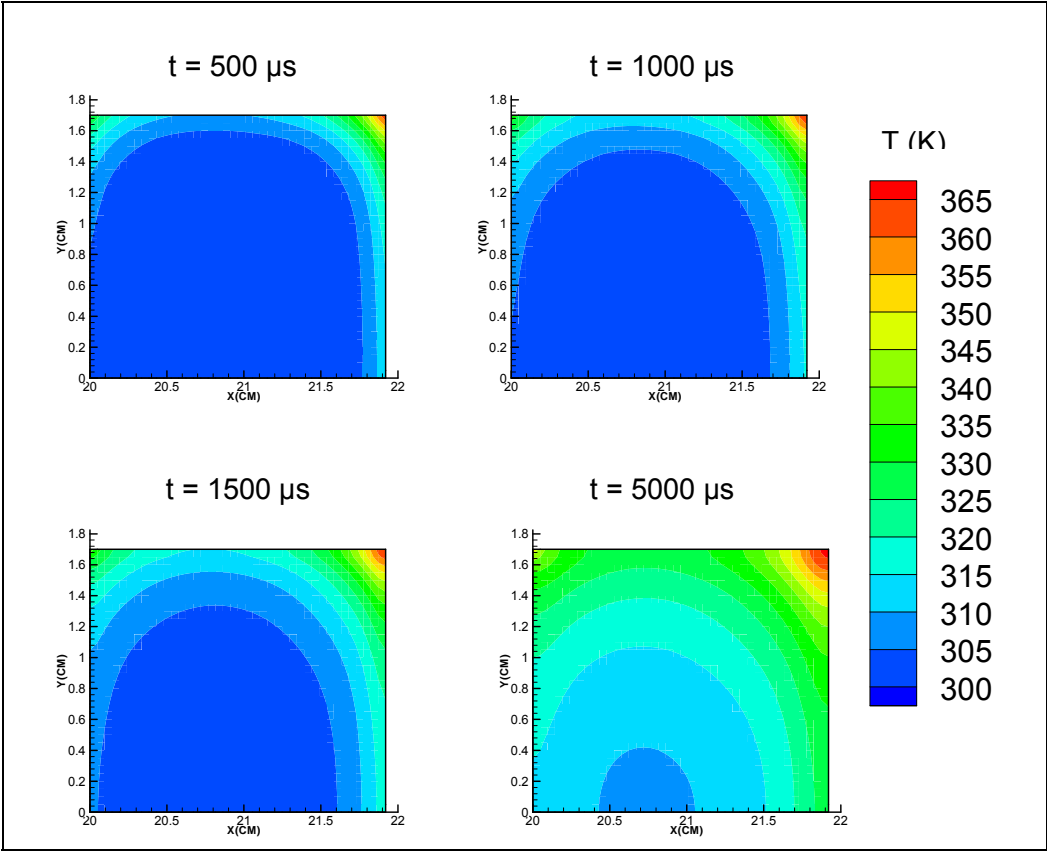


Figure 6. Temperature contours at different times.

We have finally undertaken an approximate calculation of the inductance gradient L' for this geometry at several times. This quantity can be represented as (Knoepfel, 1970)

$$L' = \frac{4}{\mu i^2} \iint B^2(x, y) dx dy, \quad (29)$$

where the integral is to be extended over the entire domain \mathcal{D} . Values for L' at various times (times correspond to those in figures 3 and 4) are shown in table 2. As might be expected, L' increases as the current diffuses inward from the sides of the rail. Kerrisk (1981) has presented formulas for L' in the high-frequency limit or, equivalently, at very early times when the current is still confined to the rail surfaces. For the present configuration, Kerrisk's formulas predict $L' = 0.56 \mu\text{H/m}$. Similarly, Grover (1946) has obtained formulas that apply for late-time, steady-state conditions when the current is uniform throughout the rail cross section. His results predict $L' = 0.67 \mu\text{H/m}$. Results in table 2 lie between these two extreme values, as should be expected. We should point out that we did not obtain results that approached Kerrisk's value at very early times. We believe, however, that this discrepancy arises from inadequate resolution of the current density near the corners when the current is largely confined to that location. Indeed, if we decreased the grid spacing in these regions, more satisfactory results were obtained. This problem will be addressed in more detail in subsequent work.

Table 2. Inductance per unit length at various times.

$t(\mu\text{s})$	$L' (\mu\text{H/m})$
200	0.591
500	0.598
1000	0.615
1500	0.627
5000	0.650

4. Summary and Future Work

We have extended a previously developed 2-D model to account for the situation in which there are two components of the magnetic induction and one component of the current density. The basic formalism was established, and the model was used to undertake one simple calculation. The calculation is concerned with the diffusion of current into a pair of infinitely long parallel rails. The configuration approximates diffusion in the rails of a railgun at distances sufficiently far behind the armature.

In future efforts, this model could be used, for example, to investigate the launch or deceleration of metallic plates by EM fields or rail erosion in railguns. For the latter problem, it will likely be necessary to include the trailing edge of the armature and to account in some approximate way for localized heating caused by the velocity skin effect. Such a calculation will extend the model beyond its rigorous range of applicability, but it may offer some insight into how erosion occurs.

5. References

- Ames, W. F. *Numerical Methods for Partial Differential Equations*; Academic Press: New York, 1977.
- Anderson, D. A.; Tannehill, J. C.; Pletcher, R. H. *Computational Fluid Mechanics and Heat Transfer*; McGraw-Hill: New York, 1984.
- Freeman, J. R. *REGGIE, A 2-D Reconnection Gun Code*; SAND88-0581; Sandia National Laboratories: Albuquerque, NM, 1988.
- Grover, F. W. *Inductance Calculations Working Formulas and Tables*; Dover Publications: New York, 1946.
- Hoffmann, K. A. *Computational Fluid Dynamics for Engineers*; Engineering Education System: Austin, TX, 1989.
- Hsieh, K. T. A Lagrangian Formulation for Mechanically, Thermally Coupled Electromagnetic Diffusive Processes With Moving Conductors. *IEEE Transactions on Magnetics* **1995**, *31*, 604.
- Kerrisk, J. F. *Current Distribution and Inductance Calculations for Rail-Gun Conductors*; LA-9092-MS; Los Alamos National Laboratory: Los Alamos, NM, 1981.
- Kerrisk, J. F. *Current Diffusion in Rail-Gun Conductors*; LA-9401-MS; Los Alamos National Laboratory: Los Alamos, NM, 1982.
- Knoepfel, H. *Pulsed High Magnetic Fields*; North Holland Publishing Company: London, 1970.
- Powell, J. D. U.S. Army Research Laboratory, Aberdeen Proving Ground, MD. Unpublished calculations, 2007.
- Powell, J. D. *Current Diffusion in Complex Cylindrical Geometries*; ARL-TR-4374; U.S. Army Research Laboratory: Aberdeen Proving Ground, MD, 2008.
- Powell, J. D.; Zielinski, A. E. Current and Heat Transport in the Solid-Armature Railgun. *IEEE Transactions on Magnetics* **1995**, *31*, 645. See also *Current and Heat Transport in the Cannon-Caliber Electromagnetic Gun Armature*; ARL-MR-258; U.S. Army Research Laboratory: Aberdeen Proving Ground, MD, 1995.

- Powell, J.; Zielinski, A. E. *A Preliminary Study of Wear in the Solid-Armature Railgun*; IAT.R 0156; Institute for Advanced Technology: Austin, TX, 1997.
- Powell, J. D.; Zielinski, A. E. Observation and Simulation of Solid-Armature Railgun Performance. *IEEE Transactions on Magnetics* **1999**, *41*, 84.
- Powell, J. D.; Zielinski, A. E. *Current and Heat Transport in a Double Taper Sabot-Armature*; ARL-TR-2523; U.S. Army Research Laboratory: Aberdeen Proving Ground, MD, 2001.
- Powell, J. D.; Zielinski, A. E. Ohmic Heating in a Double-Taper Sabot Armature. *IEEE Transactions on Magnetics* **2003**, *39*, 153.
- Powell, J. D.; Zielinski, A. E. *Electrodynamics of the Rail-Armature Interface in a Solid-Armature Railgun*; ARL-TR-3663; U.S. Army Research Laboratory: Aberdeen Proving Ground, MD, 2004.
- Powell, J. D.; Walbert, D. J.; Zielinski, A. E. *Two-Dimensional Model for Current and Heat Transport in Solid-Armature Railguns*; ARL-TR-74; U.S. Army Research Laboratory; Aberdeen Proving Ground, MD, 1993.
- Press, W. H.; Flannery, B. P.; Teukolsky, S. A.; Vetterling, W. T. *Numerical Recipes*; Cambridge University Press: New York, 1986.

NO. OF
COPIES ORGANIZATION

1 DEFENSE TECHNICAL
(PDF INFORMATION CTR
only) DTIC OCA
8725 JOHN J KINGMAN RD
STE 0944
FORT BELVOIR VA 22060-6218

1 US ARMY RSRCH DEV &
ENGRG CMD
SYSTEMS OF SYSTEMS
INTEGRATION
AMSRD SS T
6000 6TH ST STE 100
FORT BELVOIR VA 22060-5608

1 DIRECTOR
US ARMY RESEARCH LAB
IMNE ALC IMS
2800 POWDER MILL RD
ADELPHI MD 20783-1197

1 DIRECTOR
US ARMY RESEARCH LAB
AMSRD ARL CI OK TL
2800 POWDER MILL RD
ADELPHI MD 20783-1197

1 DIRECTOR
US ARMY RESEARCH LAB
AMSRD ARL CI OK T
2800 POWDER MILL RD
ADELPHI MD 20783-1197

ABERDEEN PROVING GROUND

1 DIR USARL
AMSRD ARL CI OK TP (BLDG 4600)

NO. OF
COPIES ORGANIZATION

- 1 OFFICE OF NAVAL RSRCH
E D'ANDREA
CODE 352
875 N RANDOLPH ST
ARLINGTON VA 22203-1995
- 2 INST FOR ADVNCD TCHNLGY
THE UNIV OF TEXAS
AT AUSTIN
K HSIEH
I MCNAB
3925 W BRAKER LN
AUSTIN TX 78759-5316
- 1 NORTH CAROLINA
STATE UNIV
DEPT OF NUCLEAR ENGR
M BOURHAM
BOX 7909
RALEIGH NC 27695-7909
- 2 US ARMY TACOM ARDEC
FSAE GCSS TMA
J BENNETT
D LADD
BLDG 354
PICATINNY ARSENAL NJ 07806-5000

ABERDEEN PROVING GROUND

- 24 DIR USARL
AMSRD ARL WM BA
G KATULKA
AMSRD ARL WM BD
M DEL GÜERCIO
B FORCH
A MICHLIN
A ZIELINSKI (5 CPS)
AMSRD ARL WM MB
J TZENG
AMSRD ARL WM TA
M KEELE
AMSRD ARL WM TE
P BERNING
C HUMMER
T KOTTKE
J POWELL (5 CPS)
B RINGERS
E SCHMIDT
G THOMSON
C UHLIG
G VUNNI

INTENTIONALLY LEFT BLANK.